Durability Based Service Life Estimation for Chloride Exposed Cracked and Self-Healed Concrete

Nele De Belie[1], Bjorn Van Belleghem[1], Sylvia Keßler[2], Philip Van den Heede[1] and Kim Van Tittelboom[1]

[1] Magnel-Vandepitte Laboratory for Structural Engineering and Building Materials, Ghent University, Technologiepark Zwijnaarde 60, B-9052 Ghent, Belgium, nele.debelie@ugent.be

[2] Helmut-Schmidt-University, Chair of Engineering Materials and Building Preservation, Holstenhofweg 85, Hamburg, 22043, Germany, sylvia.kessler@hsu-hh.de

Abstract. *Chloride ingress in cracked concrete leads to rapid corrosion of embedded steel reinforcement and a decrease of the expected service life. Corrosion monitoring experiments showed that a 300 µm wide crack caused initiation of corrosion of a rebar (Ø 10 mm) with a concrete cover of 26 mm within three weeks of cyclic exposure to a 33 g/l NaCl solution. After a period of unstable corrosion activity during the first 20 weeks of exposure, corrosion propagated further at a relatively high rate (0.345 to 0.718 mm³/week). Application of a theoretical pitting model revealed that a reduction of about 50% of the rebar cross-section would occur after a period of 9 to 20 years of continuous cyclic exposure to chlorides. To avoid such rapid degradation, the use of self-healing concrete can be proposed. Introduction of macro-encapsulated polyurethane into the concrete matrix, will lead to the formation of a (partial) barrier against ingress of chlorides at the moment cracks appear. Corrosion monitoring experiments showed that the autonomous crack healing could not always prevent corrosion initiation, but caused an important reduction of the corrosion rate during the 44 weeks exposure period. The mean rate of volumetric loss of steel amounted to 0.042 mm³/week, about 15 times lower than for the untreated cracked samples. The rebars also showed no or very limited signs of corrosion after visual inspection. The simplified pitting model indicated that a 50% reduction in steel cross-section would take more than 5 times longer for samples with self-healing properties versus ordinary cracked samples.*

Keywords: *Steel Corrosion, Durability, Cracking, Self-Healing Concrete, Service Life Prediction.*

1 Introduction

1.1 General Introduction

Reinforced concrete is without doubt one of the most ingenious inventions in the construction industry. By combining concrete with steel, a composite material is created which has both a high compressive and tensile strength. Numerous structures, such as buildings, bridges, tunnels and roads have been made using reinforced concrete due to its high strength and high degree of freedom in shape and design. A huge amount of steel reinforced concrete structures were built by the mid-20th century. However, these structures are now over 50 years old and several have shown major deterioration. One very common problem in reinforced concrete structures is the appearance of cracks when the concrete element is subjected to tensile stresses. These cracks form preferential pathways for chlorides or carbon dioxide to penetrate the concrete and rapidly reach the steel reinforcement. This will increase the risk for initiation and possibly further propagation of steel reinforcement corrosion. Several studies have provided proof of a

shortening of the corrosion initiation period due to the presence of cracks and chlorides (Ahmadi *et al.*, 2015; Jaffer and Hansson, 2008; B. Otieno *et al.*, 2010; Sangoju *et al.*, 2011). In some cases corrosion onset is almost instantaneous after crack appearance (Schießl & Raupach, 1997). Moreover, once corrosion has initiated, there can be an acceleration of the corrosion rate in the propagation phase as the crack provides easier supply of chlorides, moisture and oxygen to the reinforcement (Ahmadi *et al.*, 2015; Li *et al.*, 2017; Otieno *et al.*, 2010; Schießl and Raupach, 1997). Mostly, an increase in the corrosion rate was found in short term tests (< two years) while less influence of cracks on the propagation rate was found in long-term studies (Käthler *et al.*, 2017).

Thus, cracks should be repaired as soon as possible to avoid major durability issues. However, cracks in certain structures can be invisible or inaccessible, impairing repair works. Moreover, repair works have a big economic impact due to the (in)direct costs involved. Therefore, the idea of providing the concrete with the ability of restoring cracks by itself without any human interference grew during the last few decades. One promising approach to create a so-called self-healing concrete consists of the embedment of encapsulated healing agents in the concrete matrix. Brittle macro-capsules are placed in regions subjected to high tensile stresses and where cracks would cross the steel reinforcement.

In this research, autonomous crack healing through the use of encapsulated healing agents was investigated for its efficiency to reduce the ingress of chlorides into the concrete matrix and to improve the corrosion resistance of reinforced concrete.

1.2 Steel Corrosion Monitoring

Chloride ions cause breakdown of the passive layer on the steel reinforcement when present at a certain threshold concentration. As the chloride ingress in concrete is not homogenous, this leads to a very localized corrosion. Chloride induced corrosion is actually a combination of a macro-cell corrosion process (leading to a current I_{macro}) between spatially separated anodic and cathodic areas on the steel and a micro-cell corrosion process between very small anodic and cathodic parts inside the corrosion pit (leading to a current I_{micro}). The macro-cell corrosion process will usually lead to much higher corrosion rates (Schießl and Raupach, 1997). According to Ohm's law, the current which is flowing between anodic and cathodic sites on the steel surface is directly proportional to the potential difference between those areas and inversely proportional to the resistances of the system. On this basis, the macro-cell corrosion process can be represented by an equivalent electric circuit.
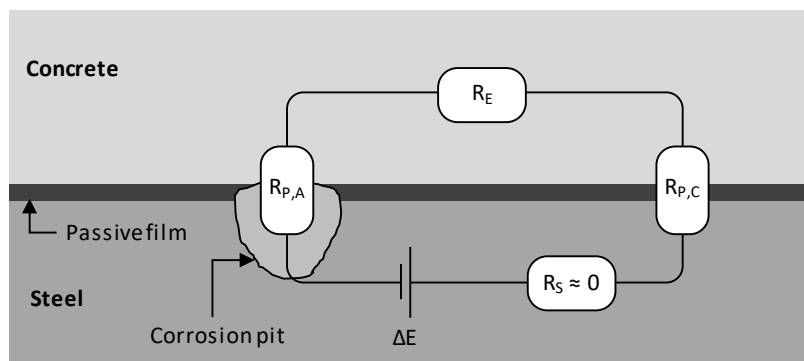

Figure 1. Equivalent circuit model for macro-cell corrosion, redrafted after Hiemer *et al.* (2015).

As can be seen from Figure 1, the equivalent circuit consists of four resistances: the resistance of the anodic partial reaction ($R_{P,A}$), the resistance of the cathodic partial reaction ($R_{P,C}$), the resistance of the concrete (R_E) and the resistance of the steel (R_S, which is assumed to be zero). The potential difference ΔE (driving potential) between the anode and the cathode can be seen as the driving force for the corrosion process. In order to estimate the rate of corrosion, the total corrosion current (I_{corr}) should be calculated, as in Equation (1).

$$I_{corr} = I_{macro} + I_{micro} = \frac{\Delta E}{R_{P,A} + R_{P,C} + R_E} + I_{micro} \qquad (1)$$

2 Materials and Methods

2.1 Concrete Samples

A reference concrete as described in Van den Heede (2014) was used as a representative mixture for concrete in exposure class XS2, i.e. submerged reinforced concrete in contact with chlorides from seawater (Table 1). The mixture had a water-to-binder ratio of 0.41 and a fly ash-to-binder ratio of 15%, according to the k-value concept (NBN B15-001, 2004). The concrete had a slump class S4 and a compressive strength at 28 days of 65.2 ± 2.0 MPa.

Table 1. Mix proportions of the concrete mixture.

Sand 0/4 (kg/m³)	696
Aggregates 2/8 (kg/m³)	502
Aggregates 8/16 (kg/m³)	654
CEM I 52.5 N (kg/m³)	317.6
Fly Ash (kg/m³)	56
Water (kg/m³)	153
Superplasticizer (ml/kg binder)	3.0

Steel reinforced concrete prisms with dimensions of 120 mm x 120 mm x 500 mm were made for corrosion monitoring. The reinforcement scheme of the prisms (Figure 1), was based on Hiemer *et al.* (2015) and Keßler *et al.* (2017), and was adapted based on earlier experiments (Van Belleghem *et al.*, 2018). The steel reinforcement (BE500S) in the concrete prisms consisted of an anodic and a cathodic part which were electrically separated from each other. The anode was a central steel bar ($\varnothing = 10$ mm, L = 250 mm), partially coated with cement paste and epoxy resin to prevent crevice corrosion, with only the central 50 mm exposed. The cathode consisted of two electrically connected cages (each with four longitudinal rebars $\varnothing = 8$ mm and five stirrups $\varnothing = 6$ mm which were welded to each other). The anode/cathode ratio was kept small (1/58) to accurately measure the macro-cell corrosion process. Both parts were connected to the exterior by means of an insulated copper wire. In addition, two glass fiber reinforced polymer rebars ($\varnothing = 6$ mm) were placed in the compression zone. Four types of specimens were prepared (with 3 replicates): uncracked specimens (UNCR), cracked but not healed specimens (CR), and self-healing specimens containing two layers of 6 capsules filled with high (6700 mPas) or low (200 mPas) viscosity polyurethane (PU_HV_CAPS and PU_LV_CAPS). The samples contained an Ag/AgCl internal reference electrode, fixed to the coated part of the anodic rebar. After casting, the prisms were stored at 20°C and a relative humidity above 95%.

The prisms were demolded after 24 hours and stored at the same conditions until 28 days. Then, anode and cathode were connected to each other through the external copper wires.
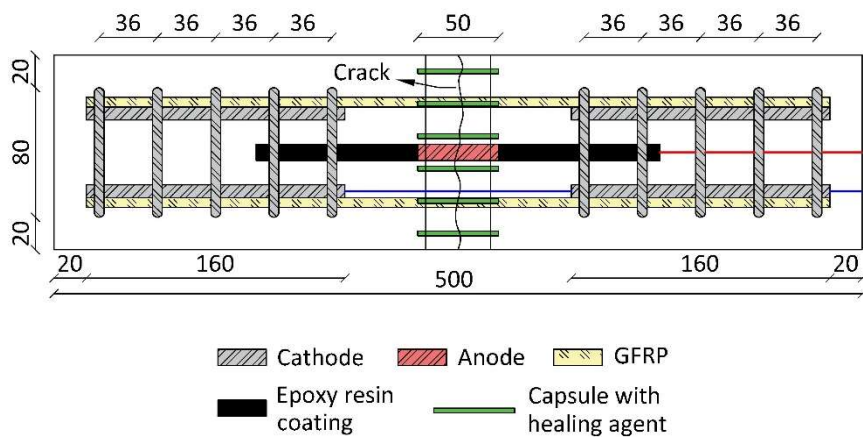

Figure 1. Reinforcement scheme and capsule positions in the concrete prisms (dimensions in mm) – top view, redrafted after Van Belleghem *et al.* (2018).

2.2 Crack Creation

At 28 days, a flexural crack with a target width of 300 µm was created in the concrete prisms by means of a three-point bending test. The concrete prisms contained a triangular notch with a height of 3.5 mm at mid-span to ensure that the cracks originated in the center of the prism and consequently crossed the anodic rebar (and the capsules). Cracks were kept open by means of a special frame (Figure 2). After crack creation, all samples were stored at $20 \pm 2°C$ and a relative humidity of 60% for 48 hours to allow the polyurethane to cure inside the crack.

2.3 Exposure Regime

The prisms were placed with the crack facing upwards and the lateral surfaces were covered with aluminum butyl tape, extending beyond the upper surface of the samples, to create a basin with three compartments (Figure 2). The top (cracked) surface of the samples was exposed weekly to 1 d wetting and 6 d drying cycles for a total duration of 44 weeks. During the wet period, the central compartment was filled with a 33 g/l NaCl solution, while the outer compartments were filled with a 1.15 g/l $Ca(OH)_2$ solution.

Figure 2. Concrete prism mounted in a three-point bending test frame (left); Basins on the surface (right).

2.4 Corrosion Measurements

The macro-cell corrosion current between anode and cathode (I_{macro}) was measured once every hour with a low resistance ammeter. Electrochemical measurements were performed at the end of the wet period with a potentiostat using the internal Ag/AgCl reference electrode (SAE). The corrosion potential (E_{corr}) was measured while anode and cathode were connected. Other parameters were measured as well (for results see Van Belleghem, 2018), such as open circuit potential (OCP) of anode and cathode, linear anodic and cathodic polarization resistance ($R_{P,A}$ and $R_{P,C}$), and concrete resistance (R_E). All electrochemical measurements were performed weekly during the first 12 weeks of the wet-dry cycles and thereafter every two to four weeks.

2.5 Chloride Profiling and Visual Evaluation

After the corrosion monitoring period, the chloride ingress was determined by means of chloride profile grinding (layers of 4 mm thickness) in an area of 10 mm x 30 mm around the crack next to the location of the anodic rebar. The total chloride content of each powder was determined by means of acid-soluble chloride extraction in a nitric acid solution followed by a potentiometric titration against silver nitrate. After determination of the chloride profiles, the anodic steel reinforcement bars were removed from the concrete prisms for visual inspection of the corrosion products. Next, all rebars were immersed in a chemical cleaner solution ($HCl:H_2O = 1:1 + 3$ g/l urotropine) for 24 hours in order to remove all corrosion products and residual concrete. Afterwards, the steel rebars were visually inspected again to investigate the loss of steel due to chloride induced corrosion.

3 Results of Corrosion Experiments

3.1 Corrosion Monitoring

An overview of the measured electrochemical parameters during the 50 weeks monitoring period is given in Figure 3. The initial measurement in the uncracked state is shown as 'week -1', while 'week 0' represents the values after cracking but without exposure to a solution. From week 1 until week 44 the samples were exposed to the wet-dry cycles. The last measurement at week 50 was performed after a six week dry period.

The uncracked samples showed a non-active state of corrosion along the whole exposure period. No macro-cell corrosion current was detected and the corrosion potential was nearly constant at values of -70 to +80 mV_{SAE}. The cracked samples showed clear evidence of corrosion initiation within the first three weeks of exposure to 33 g/l NaCl solution: there is a steep rise in the macrocell corrosion current and a concurrent drop of the corrosion potential down to values between -200 and -400 mV_{SAE}. Every week a sharp increase of the macro-cell corrosion current can be seen for all the cracked samples, which corresponds to the start of each wet period. Apart from the occurrence of these peaks, the overall macro-cell corrosion current shows a decreasing trend during the first twenty weeks of exposure. It remains relatively constant in the period from 20 to 44 weeks in a range of 20 to 60 µA, which shows that the corrosion is propagating at a constant rate. The corrosion parameters measured at week 50, after a dry period of six weeks, indicate that the corrosion is propagating at a lower rate. This is logical as the continuous supply of chlorides and moisture act as catalysts for the anodic and cathodic corrosion reaction.

Generally, the corrosion behaviour of the self-healing samples with high viscosity PU (PU_HV_CAPS) was very similar to the corrosion behaviour of the cracked samples. However, the self-healing samples with low viscosity PU (PU_LV_CAPS) behaved more closely to the uncracked samples. The macro-cell corrosion current was negligible and the driving potential was comparable to the values found for the uncracked samples.
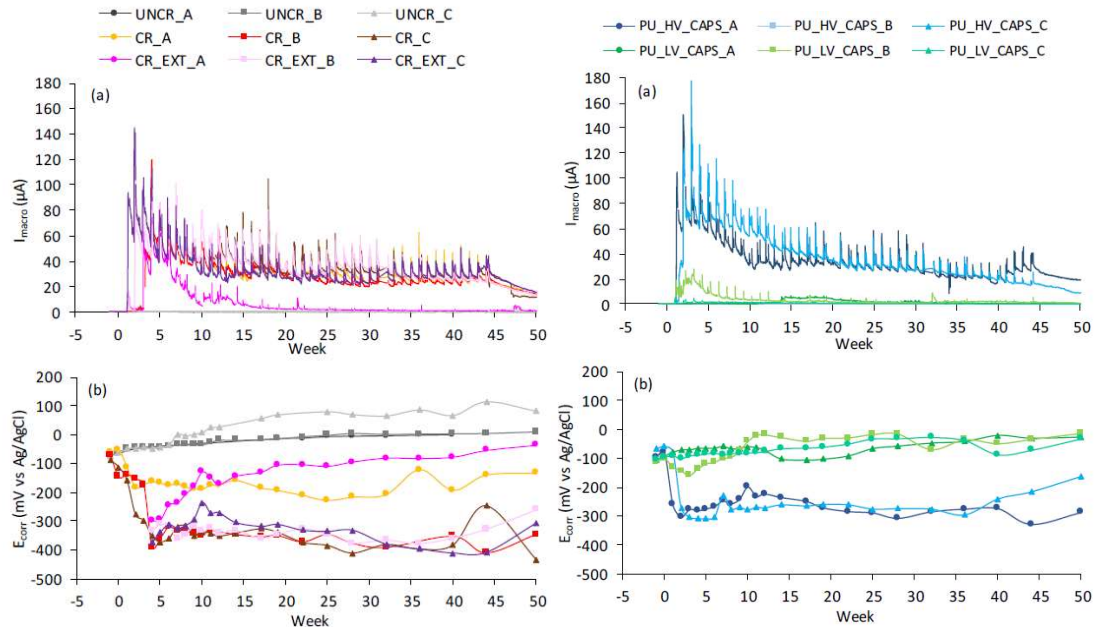

Figure 3. Macro-cell corrosion current and corrosion potential for uncracked (UNCR) and cracked (CR) samples (left) and for samples with high (HV) and low (LV) viscosity PU (right) (Van Belleghem, 2018).

3.2 Chloride Profiles and Visual Examination of the Rebars

The obtained chloride profiles are shown in Figure 4 together with the location of the rebar. For the uncracked samples the mean chloride concentration at the surface amounted to 3.43 ± 0.05 m%/binder and then dropped fast to nearly zero at a depth of 18 mm into the concrete matrix. The samples containing an untreated crack showed a very high chloride concentration close to the surface of the samples (up to 6 m%/binder). The chloride concentration drops steeply when going to the second layer (4-8 mm below the surface) and gradually decreases until a depth of 20-25 mm. At depths larger than 20 mm, the chloride concentration remained almost constant at about 1.3 to 1.5 m%/binder. Autonomous crack healing with low viscosity polyurethane (PU_LV_CAPS) led to a clear reduction of the chloride concentration compared to the cracked samples. At the level of the reinforcement the chloride concentration was about 0.26 m%/binder, which was three to seven times lower compared to the concentration found at the level of the reinforcement of the cracked samples.

Visual examination of the rebars from the uncracked samples showed no corrosion products and no visual damage to the rebars was observed after cleaning. For the cracked samples, clear formation of corrosion products on the central part of the anodic rebar was noticed. After cleaning, clear pitting corrosion was observed at the same location. The series PU_LV_CAPS showed negligible formation of corrosion products and no pitting corrosion.
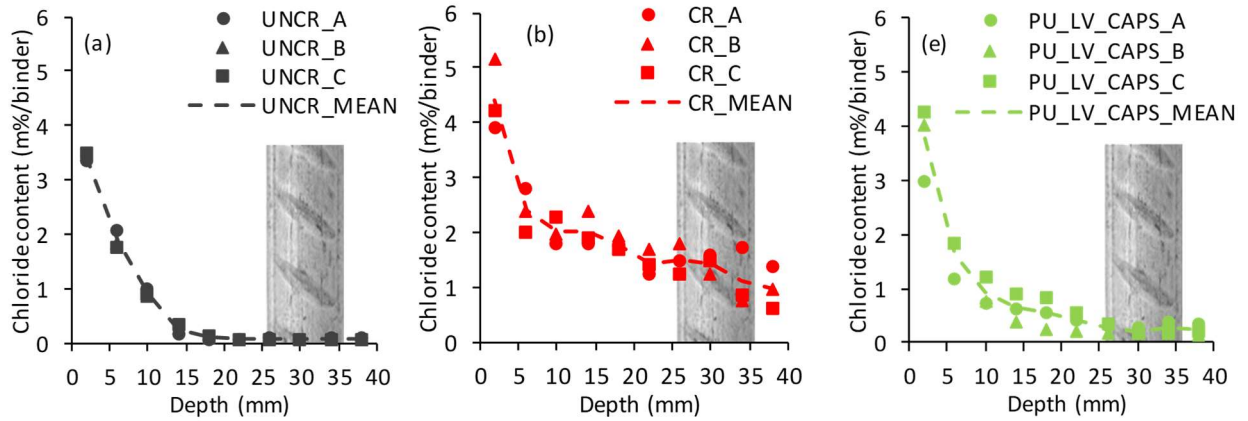
6

Figure 4. Chloride profiles of all sample series with indication of rebar location.

4 Prediction of Reduction of Steel Cross-Section

The mass loss of steel due to the macro-cell corrosion reaction can be determined theoretically from the measurement of the macro-cell corrosion current in time using Faraday's law according to Equation (2):

$$m = \frac{Q}{F} \cdot \frac{M}{z} \tag{2}$$

where m is the mass loss of iron (Fe) (g), Q is the total electric charge passed through the substance (C), F is the Faraday constant (= 96485 C/mol), M is the molar mass (here 55.845 g/mol) and z is the valency number (being 2 for oxidation of iron).

The total charge passed can be calculated by taking the integral of the measured current over time. The mass loss due to micro-cell corrosion is hereby not taken into account. The cracked samples showed a large mass loss ranging from 0.19 to 0.24 g at the end of the measurements. A further prediction can be made by calculating the volume loss in the initial 20 weeks of exposure (high and unstable corrosion current, leading to a volume loss of 6.36 to 15.45 mm³) and adding this to the volume loss in the secondary period, where a relatively stable macro-cell corrosion current develops (0.551 to 0.718 mm³/week). A similar calculation for the self-healing prisms with LV PU, resulted in an initial volume loss of 1.65 to 10.34 mm³ and a rate of volumetric loss of 0.042 mm³/week afterwards (14 times lower than what was found for the untreated cracked samples).

Application of a simplified pitting model proposed in Van Belleghem (2018) revealed that, for a steel bar with a diameter of 10 mm in cracked concrete, a reduction of about 50% of the cross-section would occur after a period of 9 to 20 years of continuous cyclic exposure to chlorides. However, for the self-healing concrete with LV PU, such a 50% reduction would take more than 100 years to occur.

5   Conclusions

- Cracks in concrete allow rapid penetration of chlorides and impair the durability of the structure. Within three weeks of cyclic exposure to a 33 g/l NaCl solution, the reinforcement in lab specimens with a 300 μm wide crack started to corrode. A volume loss of 6.36 to 15.45 mm³ was calculated for the initial 20 weeks of exposure, followed by a period of

relatively stable macro-cell corrosion current leading to a volume loss of 0.55 to 0.72 mm³/week. This means that 50% of the rebar cross-section (diameter 10 mm) would be lost after 9 to 20 years. Uncracked samples showed a non-active state of corrosion during the whole exposure period of 44 weeks.

- In the case of self-healing concrete with macro-encapsulated polyurethane, crack formation led to rupture of the capsules and release of healing agent in the crack. Low viscosity polyurethane induced a decrease of the corrosion rate in comparison to cracked and untreated samples. After an initial volume loss of 1.65-10.34 mm³, the mean steel loss rate amounted to 0.042 mm³/week only. At the end of the experiment the rebars showed no or very limited signs of corrosion. A 50% reduction in steel cross-section was estimated to take more than 100 years, using a simplified pitting model.

Acknowledgements

ORCID

Nele De Belie: http://orcid.org/0000-0002-0851-6242; Bjorn Van Belleghem: https://orcid.org/0000-0003-1294-1724; Sylvia Kessler: http://orcid.org/0000-0002-1335-1104; Philip Van den Heede: https://orcid.org/0000-0003-1307-2831; Kim Van Tittelboom: https://orcid.org/0000-0002-7718-3189

References

Ahmadi, B., Ramezanianpour, A. A. and Sobhani, J. (2015). Rebar corrosion in cracked RC prisms located in harsh marine environment. *Magazine of Concrete Research*, 66(19), 1007–1019.

Hiemer, F., Keßler, S. and Gehlen, C. (2015). Reinforcement corrosion behavior in bending cracks after short-time chloride exposure. In *Proceedings of the 4th International Conference on Concrete Repair, Rehabilitation and Retrofitting* (pp. 99–106). Leipzig, Germany.

Jaffer, S. J. and Hansson, C. M. (2008). The influence of cracks on chloride-induced corrosion of steel in ordinary Portland cement and high performance concretes subjected to different loading conditions. *Corrosion Science*, 50(12), 3343–3355.

Käthler, C. B., Angst, U., Wagner, M., Larsen, C. K. and Elsener, B. (2017). *Effect of cracks on chloride-induced corrosion of reinforcing steel in concrete – a review.* Norwegian Public Roads Administration, Report 454.

Keßler, S., Hiemer, F. and Gehlen, C. (2017). Einfluss einer Betonbeschichtung auf die Mechanismen der Bewehrungskorrosion in gerissenem Stahlbeton. *Beton- Und Stahlbetonbau*, 112(4), 198–206.

Li, W., Liu, W. and Wang, S. (2017). The effect of crack width on chloride-induced corrosion of steel in concrete. *Advances in Materials Science and Engineering*, Article ID 3968578, 11 pages.

Otieno, M.B., Alexander, M.G. and Beushausen, H. (2010). Corrosion in cracked and uncracked concrete: influence of crack width, concrete quality and crack reopening. *Magazine of Concrete Research*, 62(6), 393–404.

Sangoju, B., Gettu, R., Bharatkumar, B. H. and Neelamegam, M. (2011). Chloride-Induced Corrosion of Steel in Cracked OPC and PPC Concretes: Experimental Study. *Journal of Materials in Civil Engineering*, 23(7), 1057–1066.

Schießl, P. and Raupach, M. (1997). Laboratory studies and calculations on the influence of crack width on chloride-induced corrosion of steel in concrete. *ACI Materials Journal*, 94(1), 56–61.

Van Belleghem, B. (2018). *Effect of Capsule-Based Self-Healing on Chloride Induced Corrosion of Reinforced Concrete*. PhD thesis, Ghent university.

Van Belleghem, B., Kessler, S., Van den Heede, P., Van Tittelboom, K. and De Belie, N. (2018). Chloride induced reinforcement corrosion behavior in self-healing concrete with encapsulated polyurethane. *Cement and concrete research*, 113, 130-139.